FOURTEENTH EUROPEAN ROTORCRAFT FORUM

Paper No 46

Prediction of Inplane Damping from Deterministic and Stochastic Models

Gopal H. Gaonkar and C. S. Nagaraj
Department of Mechanical Engineering
Florida Atlantic University
Boca Raton, FL 33431-0991
U.S.A.

J. Nagabhushanam
Department of Aerospace Engineering
Indian Institute of Science
Bangalore 560 012
India

September 20-23, 1988
Milano, Italy

ASSOCIAZIONE INDUSTRIE AEROSPAZIALI
ASSOCIAZIONE ITALIANA DI AERONAUTICA ED ASTRONAUTICA

ABSTRACT

This paper reviews computational reliability, computer algebra, stochastic stability and rotating frame turbulence (RFT) in the context of predicting the blade inplane mode stability, a mode which is at best weakly damped. Computational reliability can be built into routine Floquet analysis involving trim analysis and eigenanalysis, and a highly portable special purpose processor restricted to rotorcraft dynamics analysis is found to be more economical than a multipurpose processor. While the RFT effects are dominant in turbulence modeling, the finding that turbulence stabilizes the inplane mode is based on the assumption that turbulence is white noise. The relaxation of this assumption to include RFT effects merits further research.

1. INTRODUCTION

Recently much research in "special" areas affecting the predictions of rotor blade stability has been reported. These areas include stochastic stability in turbulent flow, computational reliability and computer algebra. The term "special" is in quotes, because most of these areas merit better appreciation of their importance in the prediction process, and turbulence in particular represents extremely different points of view. Compared to recent comprehensive reviews on rotorcraft aeroelasticity [1,2], the present review is restricted to these special areas and it includes the following topics: stochastic stability and rotating frame turbulence (RFT), computational reliability of trim analysis and Floquet eigenanalysis, and comparative aspects of a multipurpose processor REDUCE and a special purpose processor DEHIM----Dynamics Equations for Helicopter Interpretive Models. Given the wide range of these topics, the review is based almost exclusively on investigations of blade

inplane stability and this facilitates presentation of these topics in a connected manner. Further, studies on inplane damping from deterministic models, following recent reviews [1,2], are briefly discussed, which also serve as a reference point for the stochastic treatments. The objective is to identify the analytical and computational strides as well as barriers toward providing a better appreciation of the special areas.

To set the stage for this review and in particular for computational reliability, a trim analysis based on periodic shooting [3] is presented. This analysis shows that for some cases, ill-conditioning could be an issue, that is, small perturbations in existing or supplied numerical data induce large changes in the computed results.

2. A TRIM ANALYSIS

For rotor systems, for which the nonlinearity is important, but not dominant, the transient and forced response are coupled in a direct way that makes Floquet theory an important tool in nonlinear dynamics. In particular, the transient dynamics (about a periodic equilibrium) depend on that equilibrium solution.

A solution strategy which couples Floquet Theory to the response analysis is the method of periodic shooting [3-5]. That method involves iterations on the initial conditions in order to find those that lead to a periodic solution of the nonlinear equations. The Floquet connection occurs in the iterative scheme. At each step of the Newton-Raphson (or secant) iteration, the partial derivatives of each deviation from periodicity with respect to each unknown (i.e., the initial conditions) are numerically computed. This process is directly related to the Floquet Transition Matrix (FTM) which similarly gives

the linearized relationship between initial values and final values. In particular, for a system with Nx1 state vector x(t) and period T,

$$\{x(T)\} = [FTM] \{x(0)\}, \{x(0)\} - \{x(T)\} = [I-FTM] \{x(0)\}$$

Thus, the matrix of partial derivatives of the errors, (x(T) - x (0)), with respect to initial conditions x(0), is I-FTM.

When control inputs are not known, the method of periodic shooting augments the vector of unknown initial conditions with unknown controls; and it simultaneously augments the vector of periodicity error with a vector of the errors in some set of desired system responses. The new matrix, which must be inverted at each iterative step, is thus larger than [I-FTM] by the number of controls (usually less than or equal to 6) and is referred to as the PDM or partial derivative matrix. In the absence of control inputs PDM reduces to [I-FTM]. The condition number (details in the next section) of the new matrix, is, therefore, of crucial importance; and I-FTM forms a large partition of it.

Figure 1 [3], illustrates the difficulty that can occur. This example is for a rigid flap-lag problem with only 4 state variables (4x4 FTM, N=4) and 4 unknown controls, m = 4. The horizontal axis is a measure of system periodicity (and nonlinearity). The vertical axis is a measure of accuracy of initial guess in the iteration. The shaded areas are initial guesses for which the Periodic-Shooting iteration does not converge. One would have expected a shaded area at high μ and low ρ, and this is the case. What one would not have expected, however, is the "fractile-like" nature of the unstable regions including a myriad of peninsulas. This points out the present problems faced in applying this method to large systems.

The erratic behavior exhibited in Figure 1 is not a function of some

$$\left\{\begin{matrix}\text{initial}\\ \text{guess}\end{matrix}\right\} = \rho \left\{\begin{matrix}\text{true}\\ \text{solution}\end{matrix}\right\}$$

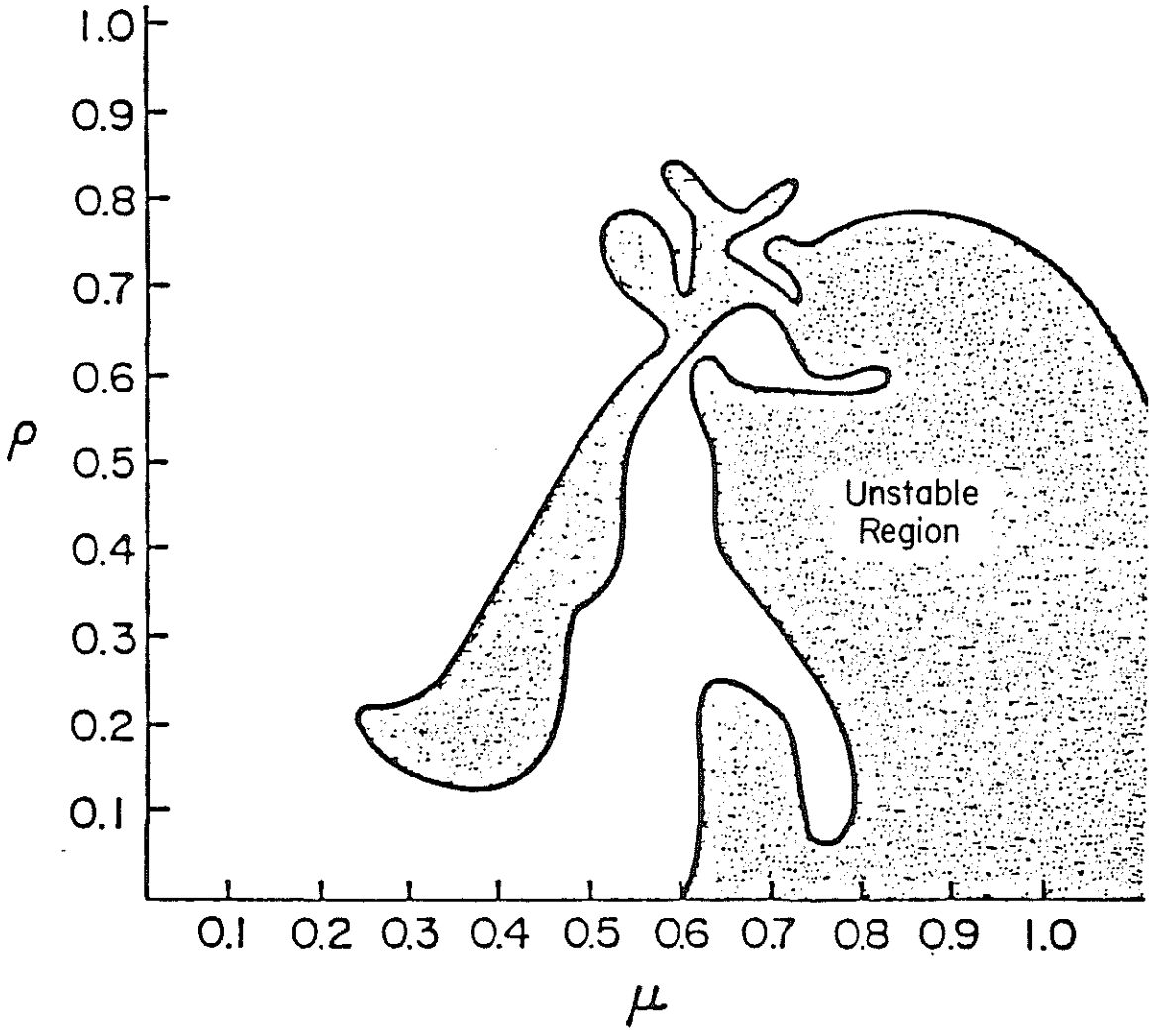

Figure 1 Convergence of Method versus Advance Ratio and Accuracy of Initial Guess.

strange nonlinearity in the system. The nonlinearities here, although important, are fairly mild and do not dominate. In this case, it was found that when applied sequentially, both 4x4 pieces converge. One might ask, "Why not, then, simply apply these iterations sequentially?" The answer is that such a strategy requires nearly 5 times as much computing time as the simultaneous or parallel algorithm [3,5]. Furthermore, it is known that the system in Figure 1 has a well defined solution, as demonstrated by the large unshaded regions and by physical considerations. Thus, a simultaneous solution strategy becomes attractive for large, practical problems, N>100. In general, no matter which strategy or method is adopted, it is important to know the condition of the problem, that is, how far small changes in the existing or supplied data affect the computed results. The condition number approach presented next provides a means of quantifying that effect and thereby quantifying computational reliability on a rigorous basis.

3. COMPUTATIONAL RELIABILITY

Application of Floquet Theory involves computation of two items [4]: 1) the periodic forced response of the system including the transition matrix for perturbations about that response and 2) a small number of eigenvalues and eigenvectors of the unsymmetric transition matrix. In addition to the initial conditions that give periodic response, unknown control variables have to be computed iteratively for desired system response; for algorithmic details of sequential or simultaneous (parallel) computations see reference 5.

In the sequel three numerical coordinates are introduced, which provide a means of routinely assessing computational reliability of Floquet analysis comprising the trim analysis and the unsymmetric eigenanalysis. Since the treatment of (mildly nonlinear) rotorcraft systems is essentially an iterative

adaptation of the linear analysis, it is convenient to begin with the Floquet analysis of a linear system.

The 2-norm is used for the vector x which can be complex and the spectral norm is used for the unsymmetric matrix A which is real. Thus,

$$\| x \| = \| x \|_2 = \sqrt{x^H x} \text{ , and } \| A \|_2 = \sqrt{(\text{max.eigenvalue of } A^T A)} \qquad (1)$$

where x^H is the Hermitian or complex-conjugate transpose of x and A^T, the transpose of A. It is good to mention that $x^H y$ represents the inner product of vectors x and y and that the vectors are normalized such that

$$\| x \| = \| x^H x \| = 1 = \| y \| = \| y^H y \| \qquad (2)$$

The condition number of matrix A or Cond.(A) is defined as

$$\text{Cond.}(A) = [\text{max. eigenvalue of } A^T A]^{1/2} / [\text{min.eigenvalue of } A^T A]^{1/2} \qquad (3)$$

A similar concept applies to any eigenvalue that is simple or of multiplicity one. If λ_j is one such eigenvalue with the left eigenvector y_j and right eigenvector x_j, then,

$$A x_j = \lambda_j x_j \text{ and } A^T x_j = \lambda_j y_j \qquad (4)$$

The significance of the quantity $\| y_j^T x_j \|^{-1}$ follows from the following relation [6]

$$\| \delta \lambda \| \leq \| \delta A \| \, \| y_j^T x_j \|^{-1} \qquad (5)$$

where $\delta\lambda$ represents the changes in λ owing to working with the matrix $A + \delta A$ instead of A. That quantity $\| y_j^T x_j \|^{-1}$ is the condition number of eigenvalue λ_j [6,7] or Cond.(λ_j). That is,

$$\text{Cond.}\ (\lambda_j) = \| y_j^T x_j \|^{-1} \tag{6}$$

It is emphasized that it is y_j^T that is used and not y_j^H. Thus Cond.(λ_j) provides a measure of the sensitivity of the computed eigenvalue λ, typified by $\delta\lambda$, to the already existing perturbations in A, typified by δA. An attractive algorithm to compute the eigenvalue condition numbers without computing eigenvectors is given in reference 8. The corresponding sensitivity analysis for eigenvectors is too involved to be practical [6] and it is expedient to use the residual error approach for the correspondent eigenpair (x_j, λ_j). From equation (4) the relative residual error ϵ is given by

$$\epsilon = \frac{\| Ax_j - \lambda_j x_j \|}{\| x_j \lambda_j \|} = \frac{\| r_j \|}{\| \lambda_j \|} \tag{7}$$

where r_j is the residual error for the correspondent eigenpair.

For a linear system with Nx1 state vector x(t) and T-periodic state matrix, the state equation is

$$\dot{x} = A(t)\ x + G(t) \tag{8}$$

where G(t) is the Nx1 forcing function. The NxN state transition matrix $\Phi(t)$ follows from the definition.

$$\dot{\Phi}(t) = A(t)\Phi(t),\ \Phi(0) = I,\ 0 \le t \le T \tag{9}$$

With $x_E(t)$ representing the nonperiodic forced response of equation (8) for zero initial state, the initial state $\{x(0)\}$ to give periodic steady state response is given by

$$\{x(0)\} = [I - \Phi(T)]^{-1} \{x_E(T)\} \tag{10}$$

For the mildly nonlinear cases of rotorcraft systems G(t) in equation (8) can be replaced by $G(x, \dot{x}, t)$ and the required initial state $\{x(0)\}$ is computed by an iterative adation of equation (10), that is, from the following equation:

$$[I - \Phi(T)]_k \ \{x_E(T) - x_E(0)\}_{k+1} = \{x_E(T) - x_E(0)\}_k \tag{11}$$

where $x_E(0)$ is an Nx1 initial state vector for some assumed initial conditions. For further algorithmic details, see references 3 and 9. For illustration, it is convenient to represent the existing vector $\{x_E(T) - x_E(0)\}_k$ by $\{b + \delta b\}$, the computed vector $\{x_E(T) - x_E(0)\}_{k+1}$ by $\{x + \delta x\}$ and the existing matrix $[I - \Phi(T)]_k$ by $[A + \delta A]$, where δb and δA represent existing errors and δx, the resulting error in the computed vector. (When control inputs are augmented with the initial conditions, as in the simultaneous or parallel strategy, $[I-\Phi(T)]$ is replaced by the partial derivative matrix PDM). The impact of the existing errors on the computed value is given by [7]

$$\frac{\| \delta x \|}{\| x \|} \le \text{cond.}(A) \left\{ \frac{\| \delta A \|}{\| A \|} + \frac{\| \delta b \|}{\| b \|} \right\} \tag{12}$$

Therefore, the larger the value of the condition number of A, the greater is the sensitivity of the computed value to existing perturbations and consequently the less well conditioned is the iteration according to equation (11). Both for the matrix condition number Cond.(A) from equation (3) and for the eigenvalue condition number Cond.(λ) from equation (6), the ideal value is one. By convention, the matrix inversion or the eigenvalue problem is said to be ill-conditioned if the corresponding condition number is larger than 100. Thus, in summary, the matrix condition number given by equation (3), the condition number of a characteristic multiplier given by equation (6) and the residual error given by equation (7) provide the three numerical coordinates, and provide a means of quantifying the computational reliability of the Floquet analysis.

The results in Table 1 [10] refer to an untrimmed rotor with 3, 4 and 5 rigid blades executing rigid flap and lag motions. The control inputs are known a priori (m=o) and the partial derivative matrix or PDM is identical to I-FTM. Thus, the trim analysis is that of finding the periodic orbit. While a 3x3 dynamic inflow feedback model is used for the three-and four-bladed rotors, a 5x5 inflow model is used for the five-bladed case. Thus the dimensions of the state vector N is equal to 15 (3x4+3), 19 (4x4+3) and 25 (5x4+5) for the three rotor models.

The first column contains the advance ratio μ and the second column, the condition number of the Floquet transition matrix FTM. The remaining three columns contain the three numerical coordinates of the Floquet eigenanalysis. All the eigenvalues were found to be simple or of multiplicity one and column 4 contains the maximum value among the N eigenvalue condition numbers. The FTM is clearly ill-conditioned and this undesirable feature increases with increasing advance ratio μ. It is remarkable that the problem of finding the periodic

Table 1: Computational Reliability Coordinates for N = 15, 19 and 25.

N = 15

μ	COND.(FTM)	COND.(I-FTM)	MAX. COND(λ)	RESIDUAL ERROR
0.0	2.79E02	1.91	1.51	0.109E-14
0.1	9.61E01	1.95	2.89	0.222E-13
0.2	6.42E02	1.89	2.32	0.165E-12
0.3	7.69E03	1.86	2.19	0.264E-11
0.4	4.50E04	1.84	2.22	0.123E-10
0.5	1.27E06	1.83	2.07	0.252E-09

N = 19

0.0	1.10E02	2.05	1.49	0.770E-15
0.1	5.59E01	2.02	3.77	0.137E-13
0.2	6.08E02	1.92	2.32	0.136E-12
0.3	7.79E03	1.88	2.13	0.146E-11
0.4	9.77E04	1.87	2.10	0.146E-10
0.5	1.36E06	1.87	2.09	0.252E-09

N = 25

0.0	3.72E02	2.05	3.40	0.272E-14
0.1	1.57E02	1.86	5.37	0.890E-14
0.2	5.94E02	1.91	3.38	0.189E-14
0.3	7.65E03	1.89	3.57	0.889E-12
0.4	9.07E04	1.87	3.39	0.273E-14
0.5	1.09E06	1.87	3.40	0.130E-14

orbit typified by equation (11) is well conditioned throughout. As seen from column 4, the problem of eigenvalue extraction is also well conditioned with respect to all the N eigenvalues. This is partially corroborated by the negligible residual error for the correspondent eigenpair (x,λ) as defined in equation (7). It was mentioned earlier that the condition number analysis for eigenvectors is too involved to be practical. The results in columns 4 and 5 show that although the condition analysis of the eigenvector computations is not included, the eigenvalue condition number in combination with the residual error provides an expedient means of quantifying the reliability of Floquet eigenanalysis.

4. COMPUTER ALGEBRA

Computer algebra is receiving increasing acceptance in generating the helicopter equations of motions [1,2,11-15]. Presently the following three approaches are used: 1) general purpose symbolic processors such as REDUCE, MACSYMA and MAPLE [12,14]; 2) a special purpose processor DEHIM---Dynamic Equations for Helicopter Interpretive Models (as used in basic research) [11,13], and 3) completely numerical schemes such as AGEM---Automatic Generation of Equations of Motions [15]. The present discussion, however, is restricted to the first two purely algebraic approaches, and specifically to a recent exercise involving the comparative aspects of REDUCE and DEHIM [10]. This exercise should be tempered by the fact the comparison of a multipurpose processor providing numerous services with a special purpose processor providing services restricted to a specialized area involves umpteen variables, many of which defy quantification [10]. Nevertheless, it should provide an improved appreciation of highly portable special purpose processors such as DEHIM.

The book by Davenport, Siret and Tournier [16] gives an excellent introduction to symbolic processing, contains extensive bibliography and also serves as a mini-user's manual for MACSYMA and REDUCE. A description of DEHIM from user's point of view is given in references 17 and 18, and reference 10 also contains a brief account of DEHIM with regard to algebraic manipulations, commands, input-output details and special features.

Table 2 shows some data from a recent study [10] in which the same set of problems were treated by REDUCE and DEHIM, as identified in the second column. Concerning the core-space requirements for installation, a special purpose processor DEHIM has significant advantage over a multipurpose processor REDUCE; 83 versus 1573, and this is expected. While column describes the nature of equations, columns 3 and 4 contain the machine time or CPU data in seconds. It is seen that the advantage of DEHIM over REDUCE concerning machine time rapidly increases with increasing system dimension.

5. TURBULENT FLOW FIELD

Rotorcraft encounter turbulent flows owing to atmospheric and self-induced turbulence. The treatment of response statistics of a deterministic linearized model subject to turbulence excitations, is a fairly routine exercise, since the treatment involves non-parametric excitations [19]. It is implied here that a trim position, a rotorcraft model linearized about that trim position and a statistical turbulence description such as input covariance matrix for excitations at different blade stations are known. However, a more realistic modeling of rotorcraft in the vicinity of turbulence leads to a system with both parametric and non-parametric excitations. For this latter case, the stability and response analyses are more demanding analytically and computationally. For

Table 2: Applications of DEHIM and REDUCE (Vax 8800)

Approach		REDUCE	DEHIM
Core Space (in blocks)		1573	83
CPU time (in secs.)			
NONLINEAR EQUATIONS (Single-Bladed Rotor)	Rigid Flap (N=2)		
	Hover	6.06	1.74
	Forward Flight	7.14	2.11
	Rigid Flap-lag(N=4)		
	Hover	9.02	5.25
	Forward Flight	12.00	8.26
LINEAR EQUATIONS (Single-Bladed Rotor)	Rigid FLAP (N=2)		
	Hover	6.59	2.81
	Forward Flight	8.16	3.25
	Rigid Flap-lag(N=4)		
	Hover	15.82	6.43
	Forward Flight	34.20	7.91
MULTIBLADE EQUATIONS (Three-bladed rotor)	Rigid Flap(N=6)		
	Hover	11.17	3.15
	Forward Flight	19.18	3.54
	Rigid Flap-lag(N=12)		
	Hover	139.00	9.06
	Forward Flight	362.00	14.39

example, stability in some probabilistic sense is governed by the state matrix containing both deterministic and stochastic terms, and the deterministic model can be recovered as a special case of the stochastic model.

Among the several definitions of stochastic stability such as stability in probability and stability with probability one (almost sure stability), the stability in the second moment or the mean-square stability is advocated for rotorcraft [20]. There are two reasons for this. First, the stability in probality and almost sure stability are difficult to apply generally, and this is particularly true of rotorcraft which represent highly coupled non-conservative systems of large dimension. Further, the mean-square stability guarantees stability in probability. Second, the stability in the first moment or the first moment stability is easy to apply since it requires only an N-dimensional Floquet analysis, where N is the dimension of the state vector. However the first-moment stability does not preclude the occurrence of high-level positive and negative transient responses from the average position. Therefore, the second moment stability is advocated, though it requires a Floquet analysis of dimension $N(N+1)/2$. Further, it guarantees the first moment stability. It should be mentioned that the first moment stability is a necessary condition for the second moment stability. More importantly, the simplicity of the first moment stability analysis often helps explain the results from the second-moment stability analysis.

Figure 2 [21] shows inplane damping levels versus advance ratio for a moment-trimmed one-bladed rotor. The blade is rigid with centrally-arranged restraining springs in flap and inplane motions. The stability results of the deterministic model including trim conditions are as in reference 22. These results form the base-line values for the stochastic stability results and are

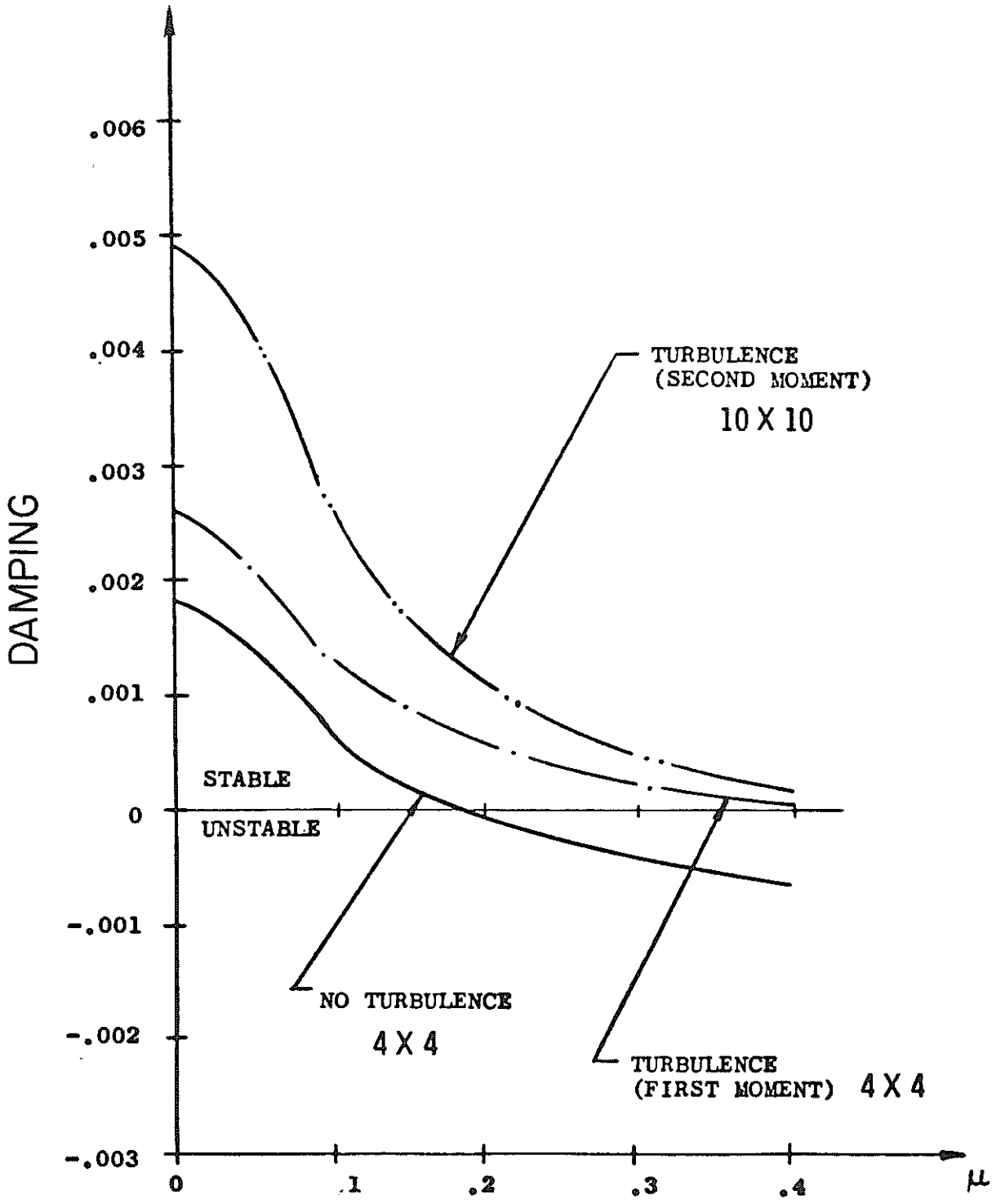

FIG. 2 EFFECT OF TURBULENCE ON BLADE DAMPING, $p=1.15$, $\omega_\zeta=1.4$, $R=0$, $\gamma=5$, $\sigma=.05$, $C_T/\sigma=.2$, TRIMMED.

referred to as no-turbulence data in figure 2. In the stochastic treatment, the basic assumptions are that the turbulence is (physical) white noise [21,23-25] and that the fore-to-aft, side-to-side and vertical turbulence velocities are uncorrelated. For the mathematical details see reference 26. Appendixes A and B of that reference give an account of the mathematical tools used in stochastic stability analysis such as stochastic averaging to obtain Ito stochastic equations.

The stochastic analysis [21,23-25] shows that the inplane stability is virtually governed by vertical turbulence velocities $\{w(t)\}$. Since $\{w(t)\}$ is approximated as white noise, the non-dimensional spectral density function S_w is constant such that

$$E\,[w(t)\; w(t+\tau)] = S_w\; \delta(\tau) \tag{13}$$

where E is the ensemble average and $\delta(\tau)$ is Dirac delta function. Henceforth, the vertical turbulence velocities $\{w(t)\}$ will be simply referred to as vertical turbulence, and S_w, as turbulence intensity.

The damping levels according to the first moment and second moment (mean square) stability criteria, as presented in figure 2, are for some assumed values of turbulence intensity. It is reiterated that while the deterministic and first moment stability analyses require an N dimensional Floquet analysis, the second moment stability anlaysis requires a Floquet analysis of dimension $N(N+1)/2$. These dimensions of the Floquet transition matrices 4 x 4, 10 x 10 etc. are also indicated in figure 2. Figure 2 points to a remarkable finding, that is, turbulence consistently stabilizes the inplane mode. This finding is further exemplified in figure 3 which shows the mean square stability boundaries in the p-ω_ζ plane for advance ratio μ = 0.3 and 0.4, where p is the flap fre-

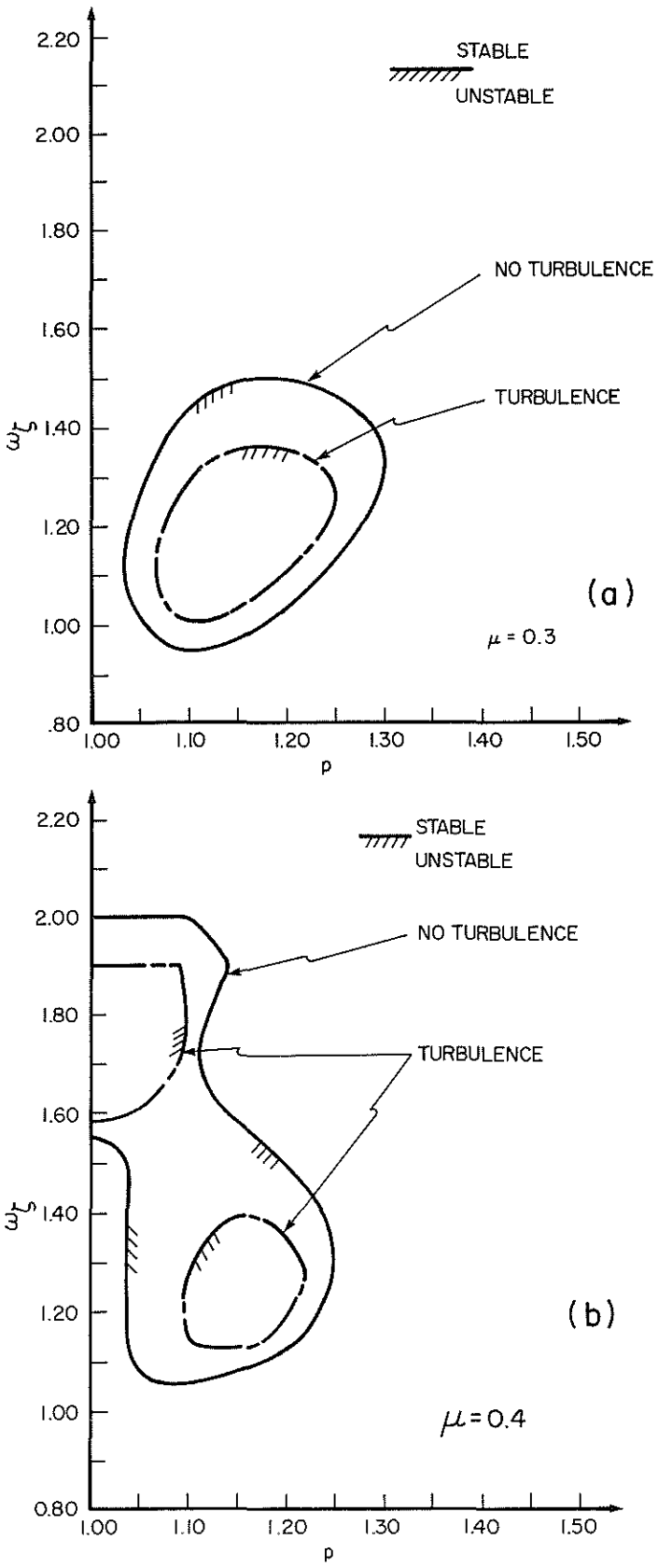

FIG. 3 STABILITY BOUNDARIES IN TERMS OF FLAP AND LEAD-LAG FREQUENCIES FOR $\mu = 0.3$ AND $\mu = 0.4$.

quency and ω_ζ, the inplane frequency. Here also the stabilizing influence of turbulence is evident. In fact, the inplane mode becomes more and more stable with increasing levels of turbulence intensity S_w, and for sufficiently high values of S_w, the instability region disappears completely. That turbulence can stabilize certain modes which were found to be unstable according to deterministic criteria is reported in the literature for simplified cases [27]. A partial explantation of this stabilizing aspect is given in reference 24 for the relatively more involved case of flap-lap stability in hover. The basis of this explanation is the first moment stability analysis which leads to an N-dimensional Floquet analysis, as does the deterministic analysis. Therefore a one-to-one comparison of damping and stiffness terms becomes possible. (By comparison, mean-square stability analysis leads to a 10 x 10 state matrix and such a comparison is not possible.) The first moment analysis with a consistent ordering scheme($1 + \epsilon^2 = 1$, $\epsilon = 0.1$), gives the following inquality:

$$\text{Lift} \sim (\theta_0 - \phi) > 2\sqrt{2\left(\frac{C_{d_0}}{a} + S_w^*\right)} \tag{14}$$

where the collective pitch θ_0 minus the inflow angle ϕ represents an average blade angle of attack. Further C_{d_0}/a is profile drag coefficient over lift curve slope and S_w^* is scaled nondimensional turbulence intensity. For the deterministic case $S_w^* = 0$ and expression (14) reduces to the deterministic results of reference 28. Since $S_w^* > 0$, it shows that the critical value of lift causing instability is higher than it is for the deterministic case. A more direct explanation of why turbulence stabilizes the mean-square flap-lag stability in forward flight is not presently available and merits further research.

5.1 Floquet Eigenanalysis

Even relatively small order stochastic systems require high order Floquet analysis, since an N-dimensional system leads to N(N+1)/2 deterministic state equations. Owing to blade elasticity, blade-to-blade coupling etc. rotorcraft models often lead to high-dimensional systems. In other words, a system with as few as 10 degrees of freedom (N=20), would lead to a 210 x 210 Floquet transition matrix which is unsymmetric. In fact many current research models have degrees of freedom well in excess of 20. The QR-Method is almost exclusively used for Floquet eigenanalysis due to its reliability and well-documented computer codes. However, it must be emphasized that the machine time requirement grows cubically with the order of the matrix, since its algorithamic structure is for a complete eigenanalysis, whereas the Floquet eigenanalysis requires in practice only a very few dominant/sub-dominant eigenvalues. Thus the QR-Method becomes prohibitively costly. This is a computational constraint which remains to be investigated in finding a viable alternative to the QR-Method in Floquet eigenanalysis.

6. Turbulence Modeling

The current stability investigations of rotorcraft in turbulence are based on the assumption that turbulence is white noise. Since the inplane stability is virtually governed by vertical turbulence, the modeling aspect of only vertical turbulence in the rotor disk is discussed, which shows how far turbulence deviates from the white noise. Here, the emphasis is on turbulence as actually felt by a rotating blade, what is referred to as rotating frame turbulence or RFT [29]. Compared to the conventional space-fixed description, the RFT requires a non-Eulerian and rotationally-sampled description [29]. This discussion is followed by a mention of the analytical constraints in relaxing the assumption that turbulence is white noise.

Recent analytical and experimental investigations [30-32] of wind turbines show that turbulence decisively influences design and operations of wind turbines. Though similar experiments are not available as yet, the importance of turbulence in rotorcraft design and operations is being increasingly recognized. While the Dryden model is widely used in rotorcraft handling qualities studies [33], most of the gust-response studies are based on the exponential model [19,29,34]. Therefore, the impact of RFT is described with respect to both the models. For horizontal-axis wind turbines, the horizontal turbulence component or the component perpendicular to the turbine disk is the most dominant component, anlogous to the vertical turbulence in rotorcraft. Figure 4 [30] shows the APSD or the auto power spectral density function of the horizontal component from rotationally sampled data (as actually measured at a blade station in a rotating frame). Figure 4 also includes the predictions from the three models without and with RFT effects. While the predictions without RFT effects refer to space fixed description, the predictions with RFT effects refer to rotationally-sampled description. The APSD with RFT effects exhibits peaks at 1P, 2P etc., and dramatically improves the correlation in capturing all the features of the test data. Given the constant energy of the spectrum, the transfer of energy with associated peaks from the low frequency region to the high frequency one is significant. It is emphasized that such peaks cannot be captured in the space-fixed description. The correlation based on the von Karman model shows that the conventional Taylor-von Karman hypothesis is viable. This is significant because this hypothesis assumes three main conditons -- stationarity, isotropy and momentarily-frozen turbulence. Although deviations from these conditions occur, (the extent of deviations depending on altitudes, nearness to obstacles and flight conditions), the overall adequacy of the Taylor-von Karman theory is remarkable and this adequacy is assumed in virtually all the

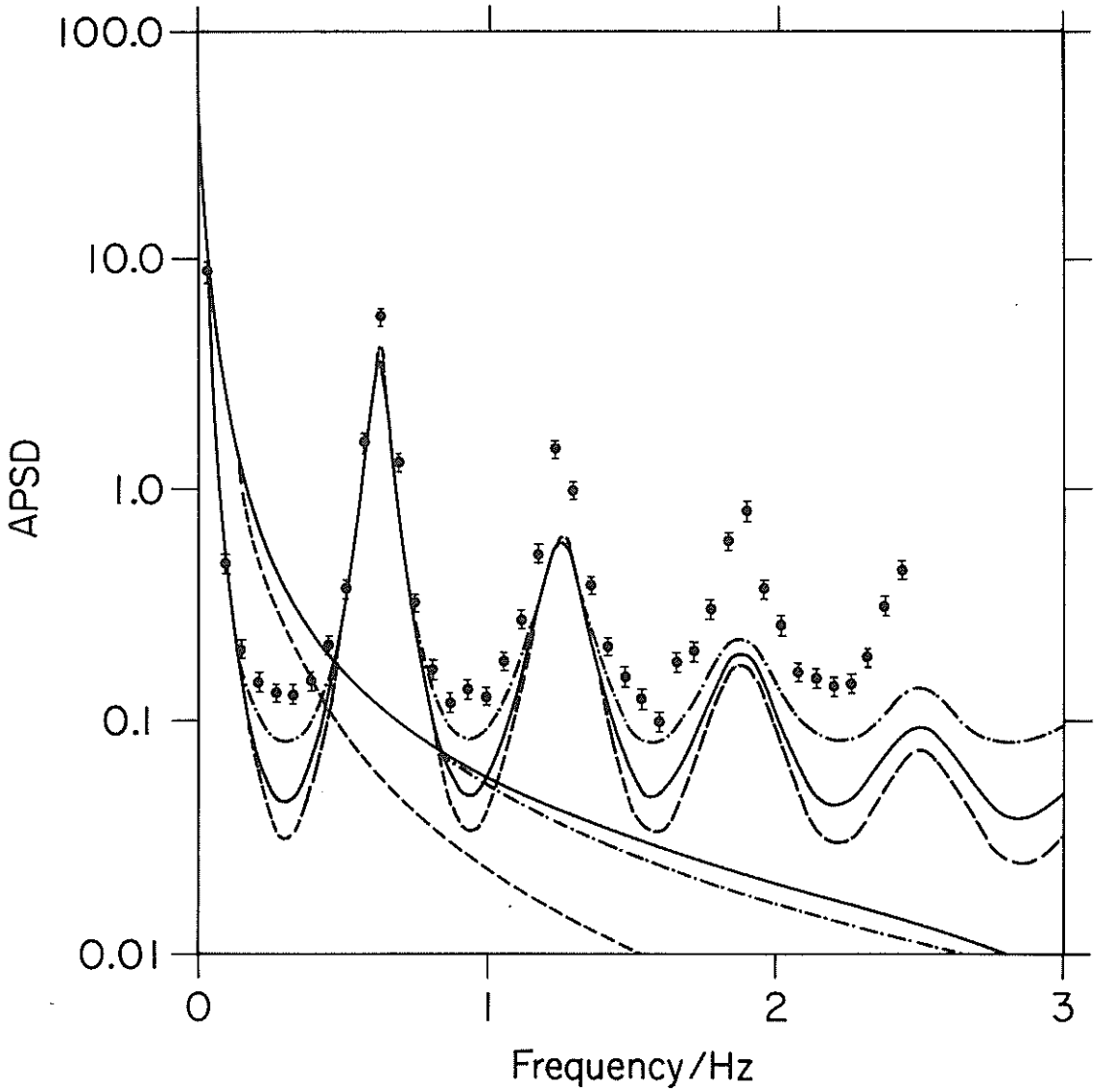

Figure 4 Spectrum of longitudinal wind speed fluctuations, as seen from a rotating blade station (RFT), compared with the space-fixed spectrum (⊕ Experimental, -·- Kaimal, — von Karman, -- Exponential)

investigations of modeling turbulence for rotorcraft and wind turbine applications.

In an attempt to explain the physics of RFT based on the Taylor-von Karman hypothesis, only the dominant vertical turbulence at one blade station, 0.7R from the rotor center, will be considered, see Figure 5. Therefore, the autocorrelation function $R_w(t_1, t_2)$ of the vertical turbulence velocities $\{w(t)\}$ is a function of the spatial separation or correlation distance r in time interval t_2-t_1. Thus,

$$R_w(t_1,t_2) = \sigma_w^2 g(r) \tag{15}$$

where σ_w is the standard deviation of $\{w(t)\}$. From Figure 5, the following is easily verified:

$$r = \sqrt{[\{X(t_2) - X(t_1)\}^2 + \{Y(t_2) - Y(t_1)\}^2 + \{Z(t_2) - Z(t_1)\}]^2} \tag{16a}$$

$$X(t_2) - X(t1) = V(t_2-t_1) + 0.7\ \Omega R\ (\sin \Omega t_2 - \sin \Omega t_1) \tag{16b}$$

$$Y(t_2)- Y(t_1) = 0.7\ \Omega R\ (\cos \Omega t_2 - \cos \Omega t_1) \tag{16c}$$

$$Z(t_2) - Z(t_1) = U(t_2)-U(t_1) \tag{16d}$$

In equation (16d), U is the total mean air-flow velocity in the Z direction due to axial flight velocity, mean vertical turbulence velocity and downwash. For the numerical results discussed here U is set to equal to $k\lambda\Omega R$ where k is a scaling constant, λ, total inflow and ΩR, the tip speed. If L is the turbulence scale length for the longitudinal turbulence component, L/2 is the scale length for the vertical component [19]. For advance ratio μ, the nondimensional spatial separation r/(L/2) from equations (15) and (16) can be expressed as

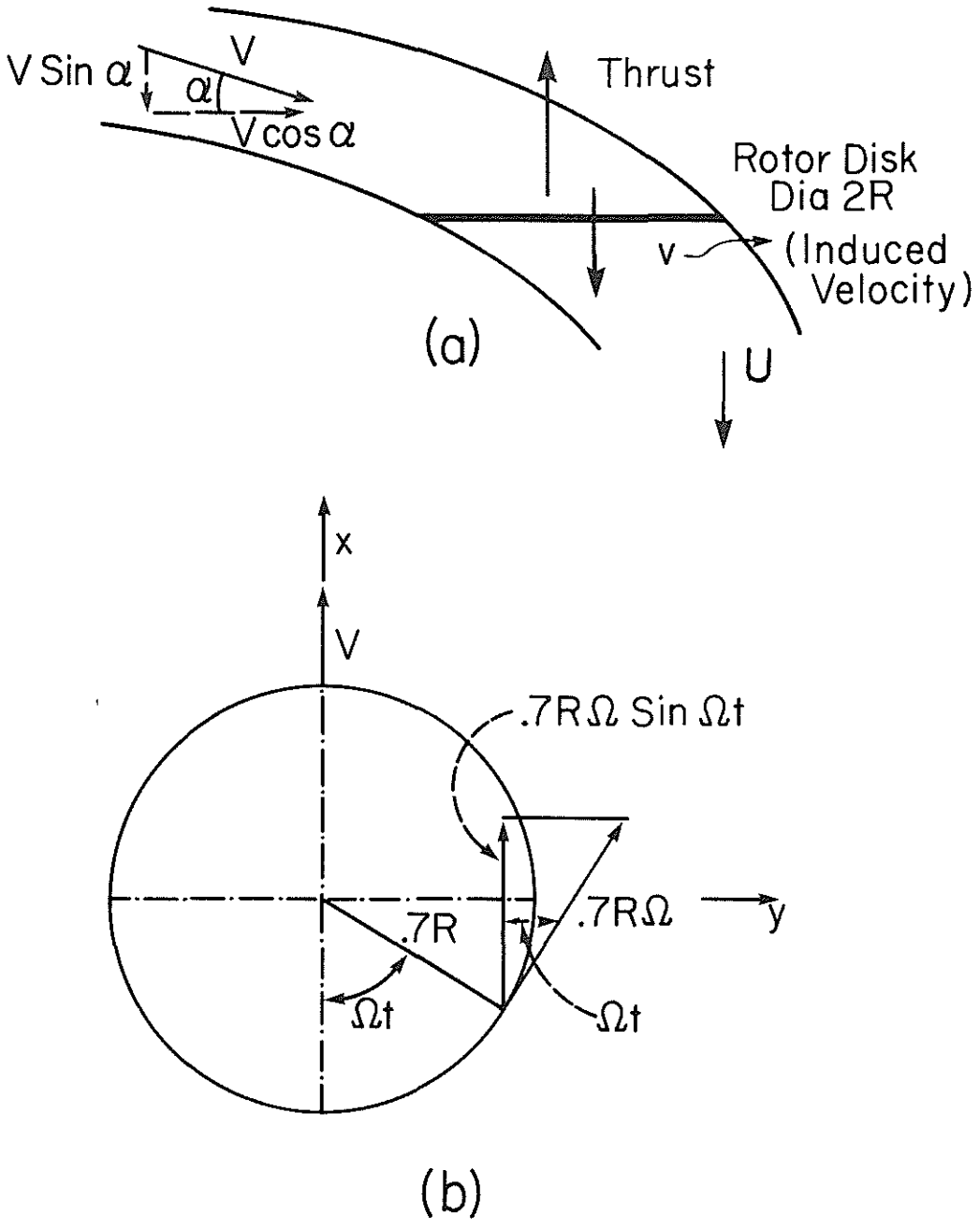

Figure 5 Rotor in forward flight (momentum theory)

$$r/(L/2) = [\{(\mu R/(L/2)\ (\bar{t}_2-\bar{t}_1) - (0.7R/(L/2))\cos\bar{t}_2 + (0.7R/(L/2))\cos\bar{t}_1\}^2$$

$$+ \{(0.7R/(L/2))\sin\bar{t}_2 - (0.7R/(L/2))\sin\bar{t}_1\}^2$$

$$+ \{(\bar{U}R/(L/2)\ (\bar{t}_2-\bar{t}_1)\}^2]^{1/2} \qquad (17)$$

where $\bar{t}_1 = \Omega t_1$, $\bar{t}_2 = \Omega t_2$ and $\bar{U} = U/\Omega R$.

To study the stationary and nonstationary aspects, it is convenient to introduce the change of variables such that $\bar{t}_2 - \bar{t}_1 = \tau$ and $(\bar{t_1} + \bar{t}_2)/2 = t$. With the definitions $a = \mu/(L/2R)$, $b = \bar{U}/(L/2R)$ and $c = 0.7/(L/2R)$, equation (17) simplifies to

$$r/(L/2) = [\tau^2\ (a^2+b^2) + 4c \sin\tau/2\ (c \sin\tau/2 + a\tau \sin t]^{1/2} \qquad (18)$$

Equations (15) and 18) show that turbulence in the rotor disk is stationary for c=o or for a=o. The first condition, c=o, implies neglect of RFT effects. In other words turbulence as existing at the rotor centre is the representative sample of the entire disk. The second condition, a=o, shows that the turbulence is stationary under axial flight conditions (μ=o) even with inclusion of RFT effects.

The widely-used Dryden model has the following spectral density function:

$$S_W\ (\omega) = \sigma_W^2\ \frac{L}{\pi}\left[\frac{1+3L^2\omega^2}{(1+L^2\omega^2)^2}\right] \qquad (19)$$

where ω is the spatial frequency. The inverse Fourier transform of equation (19) gives the autocorrelation function:

$$R_W\ (r) = \sigma_W^2\ (1 - \frac{r}{2L})\ \text{exp.}\ (-r/L) \qquad (20)$$

where r is the correlation distance given by equation (18). Figure 6 shows the spectral density function and the autocorrelation function (upper-right inset figure) according to equations (18), (19) and (20). The corresponding descriptions without RFT effects are shown by the dotted lines. The transfer of energy toward the high frequency region and the occurrence of peaks at 1P, 2P etc. are clearly evident. The impact of RFT on rigid flap response in hover is shown in figure 7. The blade lock number γ = 8 and the flapping frequency P=1.1. The turbulence description is based on the exponential model for which the autocorrelation function R_w (r) is given by equation (21)

$$R_w (r) = \sigma_w^2 \exp. (-r/(L/2)) \qquad (21)$$

The Fourier transform of equation (19) gives the corresponding spectral density function. In figure 7, the spectral density of flap response is shown without and with RFT effects. It is clearly seen that the dominant response at 1P is well captured with inclusion of RFT effects. The response peaks occur owing to energy transfer (with associated peaks) from the low-frequency region to the high-frequency region in the turbulence spectrum, see figure 6. Test data in wind turbines [31] corroborate the occurrence of such peaks in response spectra.

Figure 8 shows the autocorrelation function at 0.7R blade station with RFT effects for L/R = 1 and L/R = 4. The space-fixed description is based on the Dryden model given by equation (20). The case with μ=0.05 corresponds to transition flight and the second case with μ=0.2 corresponds to steady cruising. As seen from equation (18), the excitation with RFT effects in forward flight is nonstationary, that is, $R_w(r)$ is a function of both t_1 and t_2, and not of $(t_2 - t_1)$ only as in hover. Figure 8 is basically a two-dimensional analogue of the autocorrelation function $R_w(\tau)$ shown in figure 6 (top-right inset figure).

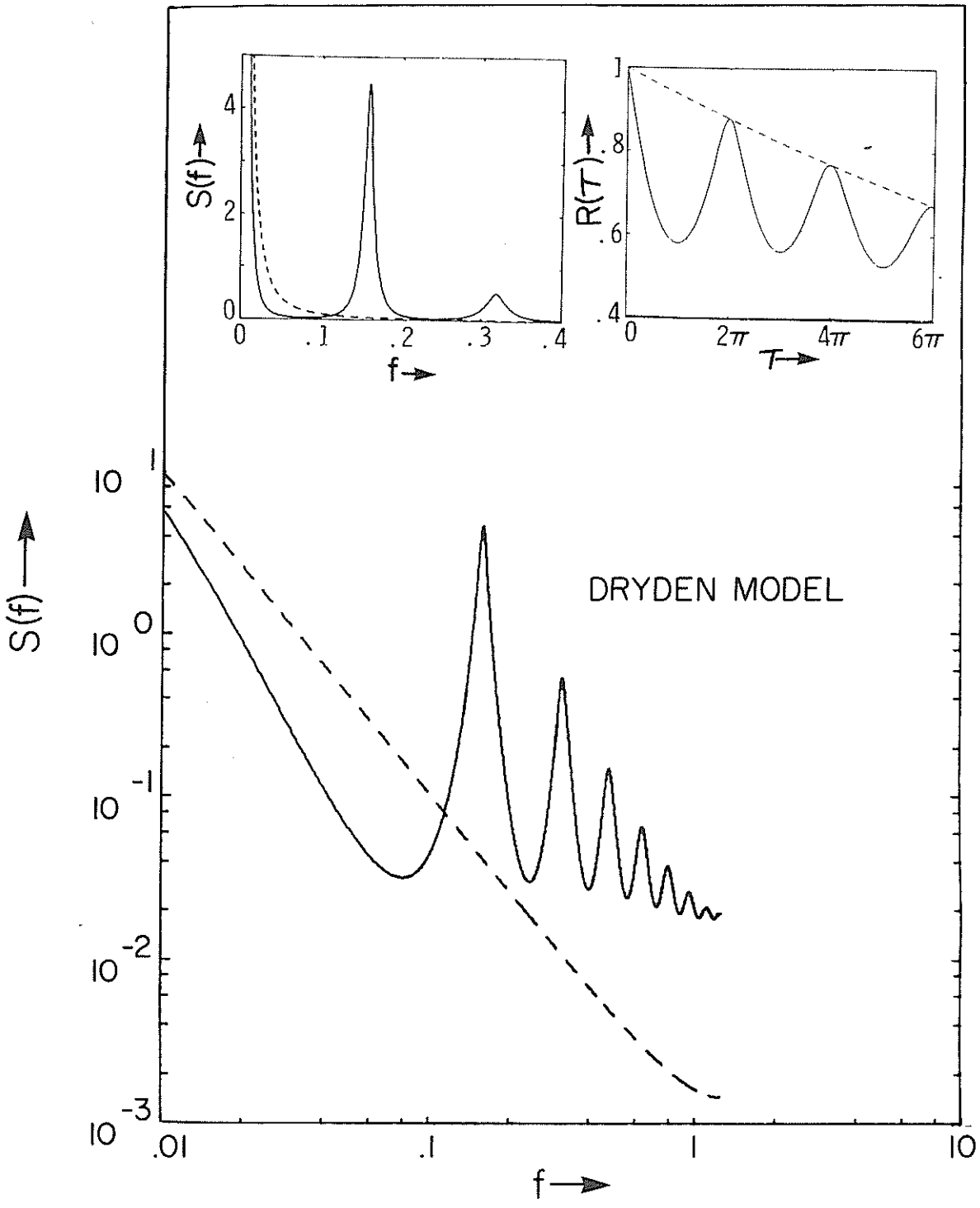

FIG. 6 RFT FOR SPACE-FIXED DRYDEN MODEL

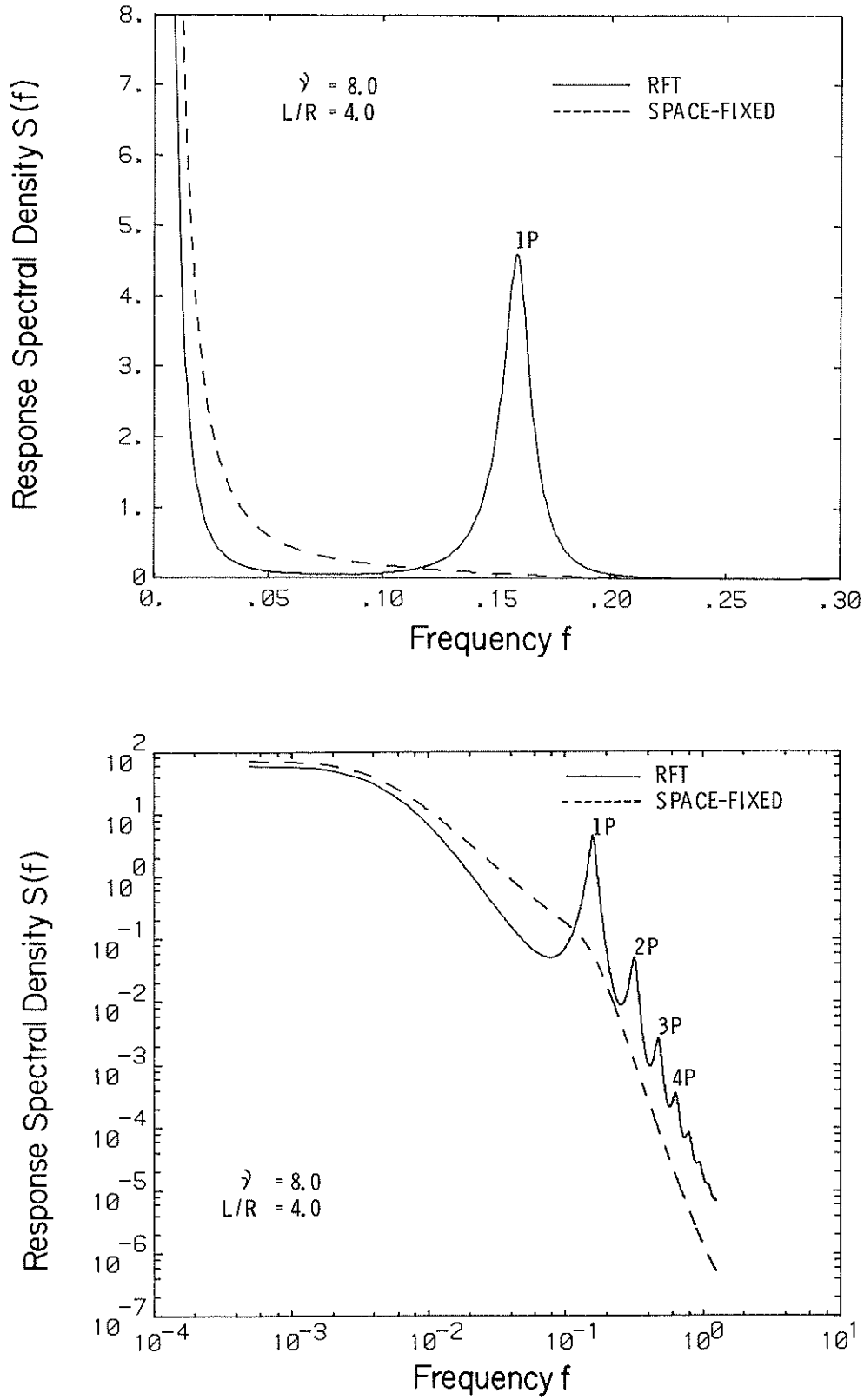

FIG. 7 FLAP RESPONSE SPECTRAL DENSITY IN HOVER FOR SPACE FIXED AND RFT EXCITATIONS FROM EXPONENTIAL MODEL.

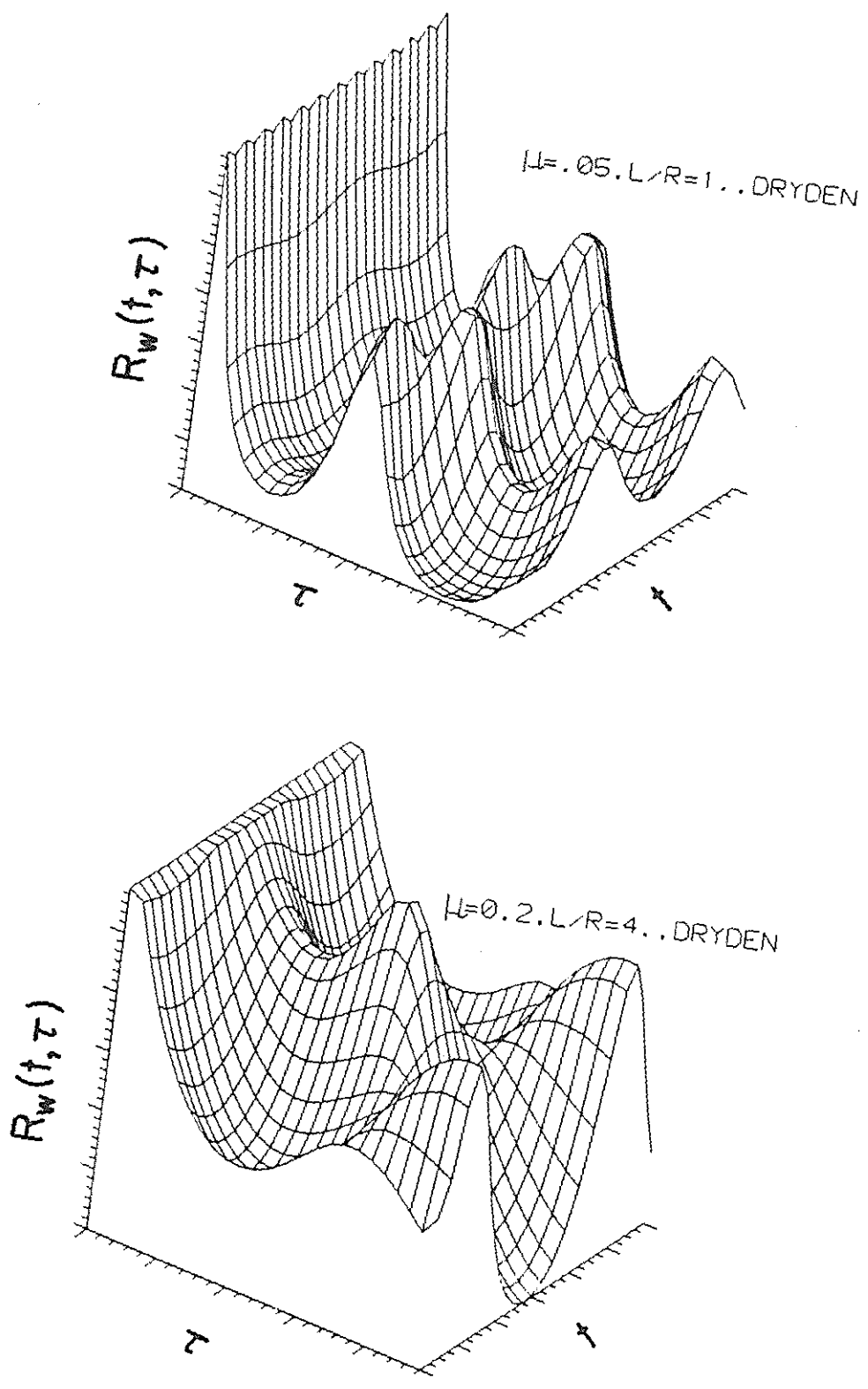

FIGURE 8 RFT IN FORWARD FLIGHT BASED ON DRYDEN MODEL

6.1 Analytical Constraints

The stochastic stability concept was first applied to rotorcraft problems in reference 26. This involves spohisticated mathematical tools of stochastic averaging and the assumption that turbulence is (physical) white noise with constant spectral density (or turbulence intensity S_W, equation 13). As seen from figures 6 and 8, the turbulence exhibits considerable deviations from the white noise model. In the case of non-parametic excitations, the shaping filter approach is a straight forward exercise in which the physical state vector is augmented with the artificial state vector of the filter equations. However, the stochastic stability investigation involves parametric excitations. Therefore, the shaping-filter approach introduces artificial nonlinearity due to multiplication of physical state variables and the artificial state variables of the filter equations. With the present state-of-the-art it is difficult to assess the reliability of the results obtained by the currently used approach in the presence of such nonlinearity. This aspect of the problem remains to be investigated.

7. Deterministic Predictions

Deterministic predictions provide the reference or base-line values for the corresponding stochastic stability treatments. Predictions of inplane damping from deterministic models merit significant refinements and are well covered in two comprehensive reviews [1,2]. Following these reviews, studies on inplane damping include reference 35 in which correlations between experimental data and predictions are presented. The predictions are based on a linear quasi-steady aerodynamics theory and on a quasi-steady stall theory which is this linear theory refined to include nonlinear airfoil-section lift and drag characteristics. A noteworthy aspect of that study concerns the stalled, high advance

ratio cases which are addressed here. For such cases, the quasi-steady stall theory was found to be qualitatively different from the linear theory, and overall, neither theory did well. Further, this qualitative difference is primarily due to non-linear lift characteristics and marginally due to non-linear drag characteristics [35]. Therefore, it is instructive to study the sensitivity of predictions to reasonable changes in the assumed nonlinear lift characteristics, as shown in figure 9. The airfoil is NACA 23012. The test Reynolds number in hover at 0.7R blade station is close to 184,000, which is used as a reference value in forward flight as well. Figure 9 shows the four types of lift characteristics including the one (figure 9a) used in reference 35. The nonlinear airfoil-section drag coefficient $C_{d_0}(\alpha)$ is identical to the one used in reference 35 and $C_{d_0,min} = 0.0079$. These characteristics are identical in substall ($|$ angle of attack $| \leq 12°$) and exhibit considerable variations for stalled conditions.

It is expedient to begin with the hovering conditions for which it was shown [36] that inclusion of quasi-steady stall characteristics dramatically improves correlation with the data from a rigid flap-lag test model. Figure 10 shows the comparison of two predictions. The predictions from reference 36 which is restricted to hovering conditions is shown by full lines. The predictions labeled 'results from present analysis' and shown by dotted lines are the results generated from the analysis of reference 35 for the test configuration of reference 36. The good agreement between these two predictions is noteworthy.

Figure 11 shows the correlation with test data for the two cases of collective pitch angles (θ_0 = 0° and 3°) in combination with a shaft tilt angle α_s = 12°. The test model represents an isolated three-bladed rotor and the spring restrained rigid blades execute flap and inplane motions. The rotor is

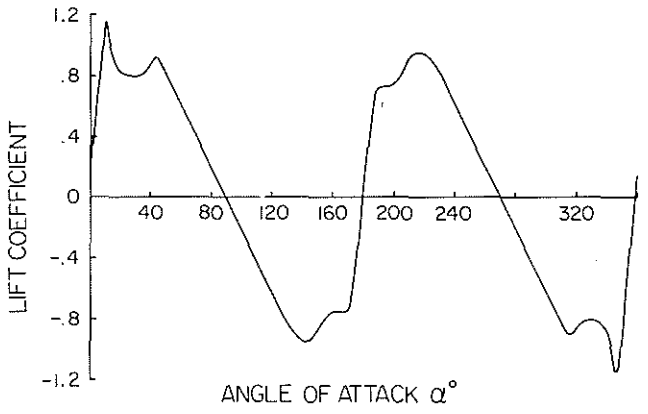

(a)

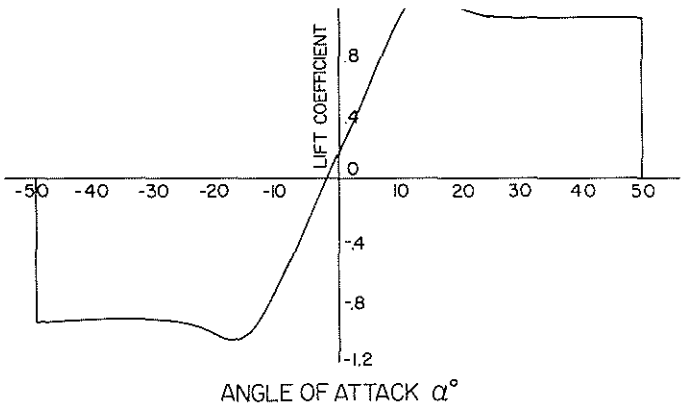

(c)

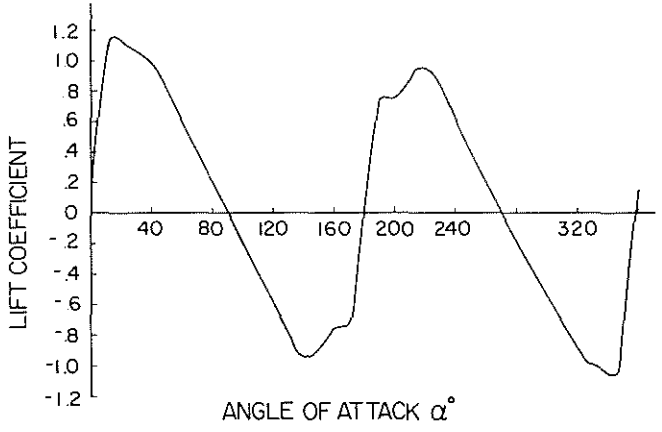

(b)

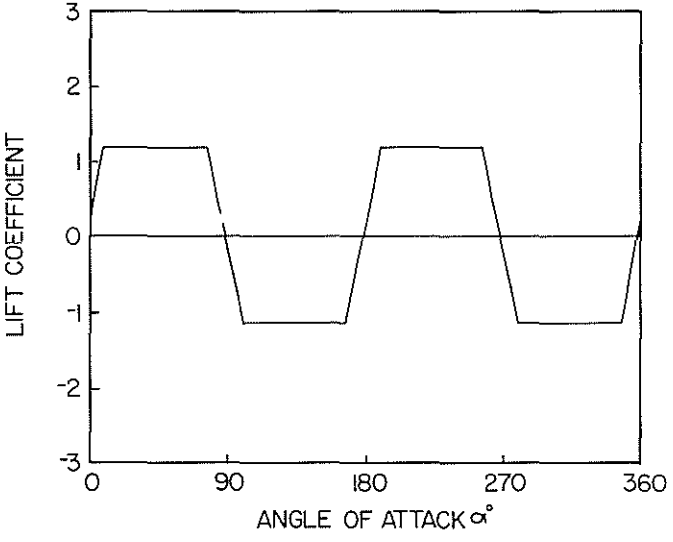

(d)

FIGURE 9 ASSUMED NON-LINEAR LIFT CHARACTERISTICS

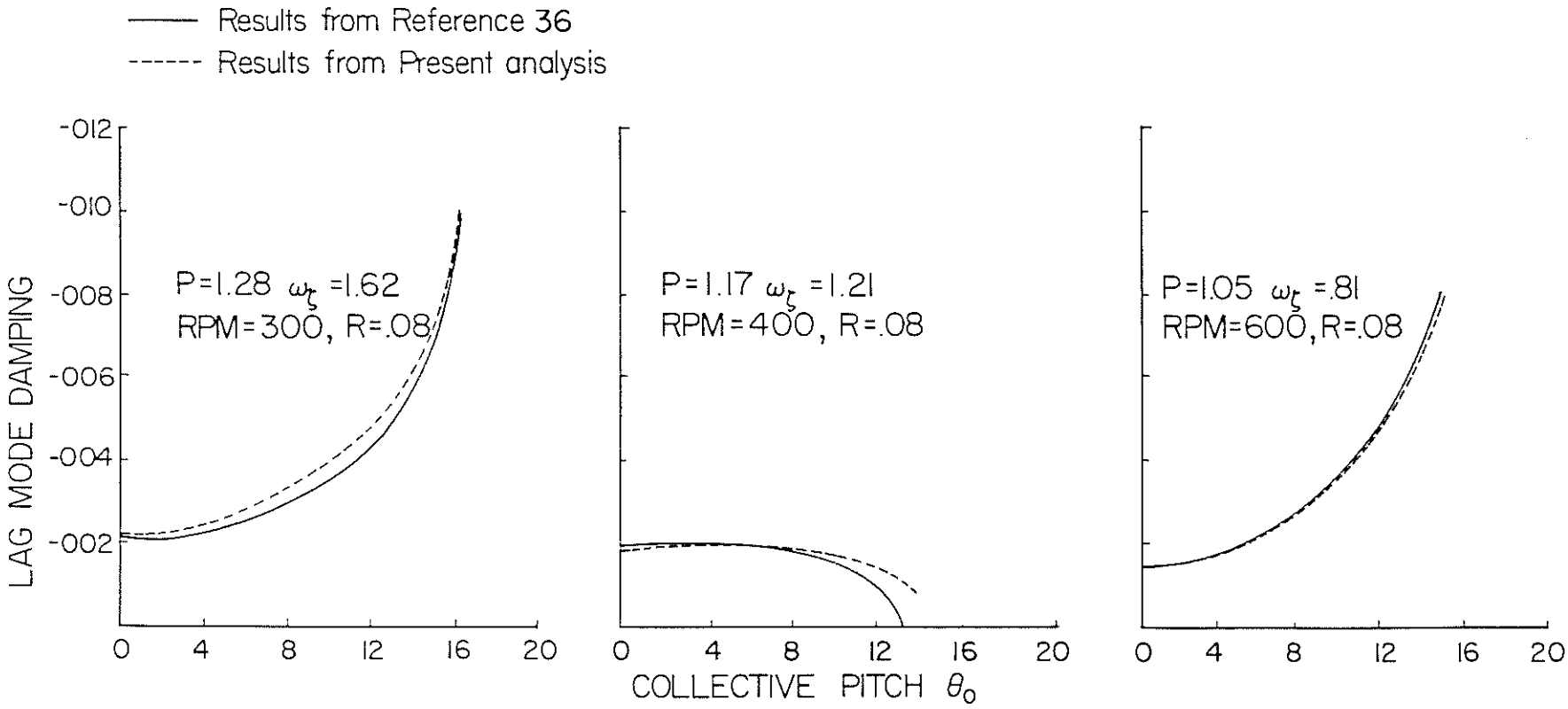

Figure 10: Comparison of two predictions

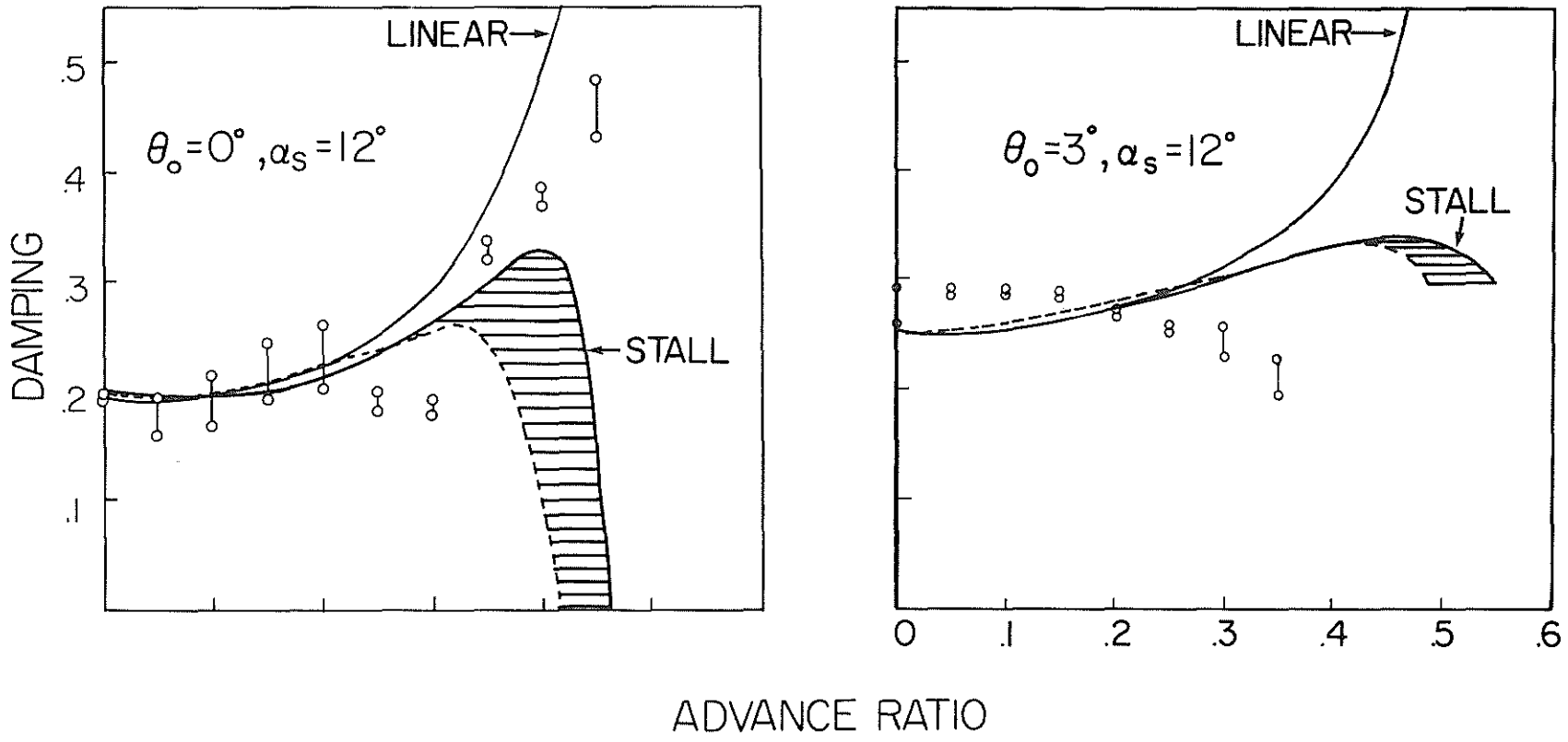

FIG. 11 RANGE OF INPLANE DAMPING PREDICTIONS AND CORRELATIONS WITH TEST DATA.

untrimmed with known collective pitch angle θ_0 and the shaft tilt angle α The structural simplicity of the rigid-hinged representation without torsion degree of freedom facilitates isolate the aerodynamic ingredients that pa ticipate in the correlation between theory and data. While the dotted li shows the predictions of reference 35 using the lift characteristics shown figure 9a, the predictions using the lift characteristics of figure 9b are sho by full lines. The other two sets of predictions using the lift characteristi of figures 9c and 9d fall in between the dotted and full lines (closer to t full line). Thus, the hatched portion in figure 11 shows the variations in t predictions for the four lift characteristics shown in figure 9. Reasonab good correlation is obtained up to an advance ratio $\mu \approx 0.25$ when, as expecte the linear theory and the quasi-steady stall theory essentially give the sa values. The minor variations are due to nonlinear drag characteristi However, with increasing advance ratio ($\mu > 0.25$), the blade experienc increasing stall effects, and the results from the quasi-steady stall theory a not consistently better than the linear theory results. Correlations shown figure 11 thus corroborate the finding of reference 35. That is, wi increasing advance ratio, both the theories become increasinly inadequate a that inadequacy is not overly sensitive to assumed lift characteristics. T stalled, high advance ratio cases are not adequately predicted by the quas steady stall theory and seem to indicate dynamic stall effects which signif cantly influences trim analysis [37]. With the present state-of-the-art it difficult to assess how far dynamic stall affects inplane damping prediction However, these differences between test data and predictions based on line theory and quasi-steady stall theory should provide the motivation to isola dynamic stall effects.

8. CONCLUDING REMARKS

1. The matrix condition number, the eigenvalue condition number and the residual error of an eigenpair (the eigenvalue and the correspondent eigenvector) provide a means of quantifying the computational reliability of Floquet analysis involving the trim analysis and the eigenanalysis. These three numerical coordinates can be built into routine Floquet analysis.

2. That the computer algebra is a desirable adjunct of rotorcraft dynamics research is increasingly recognized. Experiments with a highly portable special purpose processor DEHIM shows that it is more economical when compared to multipurpose processors such as REDUCE. These advantages should be tempered by the fact that a special purpose processor is restricted to a specialized area of research when compared to multipurpose processors which provide numerous services.

3. Stochastic stability investigations show that the inplane mode is increasingly stabilized with increasing turbulence intensity. These investigations are based on the assumption that turbulence is white noise and require a Floquet eigenanalysis of dimension $N(N + 1)/2$, where N is the system dimension. The relaxation of this assumption would introduce apparent or artificial nonlinearity, and since the reliability of the results obtained by the currently used stochastic averaging approach is not certain at the present time, this merits further research.

4. In the Floquet eigenanalysis the QR method is almost exclusively used. The algorithmic structure of this method is oriented to a complete eigenanalysis. But the unsymmetric eigenanalysis of the Floquet transition matrix requires a very few dominant/sub-dominant eigenvalues and eigenvectors. For the QR method the machine time requirement grows cubically with the

dimension of the system. Therefore, for large deterministic systems and even for relatively small order stochastic systems with parametric excitations, the QR method becomes prohibitively costly.

5. That stalled, high advance ratio cases are not adequately predicted by quasi-steady stall theory seem to indicate dynamic stall effects which significantly influence trim analysis.

6. Compared to space-fixed description of turbulence, non-Eulerian and rotationally sampled (rotating frame turbulence or RFT) descrition shows significant transfer of energy from the low frequency region to high frequency region with associated peaks at 1P, 2P etc. Such peaks cannot be captured in the conventional space-fixed description. In turbulence modeling RFT effects should be included. Neglect of RFT effects as in the space-fixed description leads to significant under prediction of response characteristics.

7. The following research areas offer considerable promise: (1) Analytical tools to treat stability of rotorcraft in turbulence by relaxing the assumption that turbulence is white noise. (2) a viable alternative to the QR Method in Floquet eigenanalysis and (3) prediction of inplane damping with dynamic stall.

9. ACKNOWLEDGEMENT

This work is sponsored by the U. S. Army Research Office under grant No. DAALO3 and by the NASA-Ames University Consortium under subcontract No. E-16-606-S1 from the Georgia Institute of Technology. The view, opinion and/or findings contained in this report are those of the authors, and should not be construed as an official Department of the Army position, policy, or decision, unless so designated by other documentation.

10. REFERENCES

1. Friedman, Peretz P., "Recent Trends in Rotary Wing Aeroelasticity", Vertica Vol. 11, No. 1/2, 1987, pp. 139-170.

2. Ormiston, R.A. et al., "Rotorcraft Aeroelastic Stability", NASA/Army Rotorcraft Technology, NASA Conference Publication 2495, March 17-19, 1987, pp. 353-529.

3. Peters, D.A. and Izsadpanah, A.P., "Helicopter Trim by Periodic Shooting with Newton-Raphson Iteration", Proceedings of the 37th Annual National Forum of the American Helicopter Society, New Orleans, May 1981, Paper 81-23.

4. Gaonkar, G.H. and Peters, D.A., "Review of Floquet Theory in Stability and Response Analysis of Dynamic Systems with Periodic Coefficients", Recent Trends in Aeroelasticity, Structures and Structural Dynamics, University Presses of Florida, Gainesville, Edited by P. Hajela, 1987, pp. 101-119.

5. O'Malley, James A., Izadpanah, Amir P., and Peters, D.A., "Comparison of Three Numerical Trim Methods for Rotor Airloads", Ninth European Rotorcraft Forum, Stresa, Italy, September 13-15, 1983, Paper No. 58.

6. Gourlay, A.R., and Watson, G.A., Computational Methods for Matrix Eigenproblems, John Wiley and Sons, New York, p. 24.

7. Ortega, J.M., Numerical Analysis: A Second Course, Academic Press, New York, 1972, Chapters 2 and 3.

8. Chan, S.P., Feldman, R., and Parlett, B.N., "Algorithm 517 - A program for Computing the Condition Numbers of Matrix Eigenvalues Without Computing Eigenvectors", ACM Transactions on Mathematical Software, Vol. 3, No. 2, June 1977, pp. 186-203.

9. Dugundji, J. and Wendell, J.H., "Some Analysis Methods for Rotating Systems with Periodic Coefficients", AIAA Journal, Vol. 21, No. 6, June 1983, pp. 390-897.

10. Ravichandran, S., Gaonkar, G.H., Nagabhushanam, J., and Reddy T.S.R., "A Study of Symbolic Processing and Computational Aspects in Helicopter Dynamics", Paper presented at the Sixth Army Conference on Applied Mathematics and Computing, May 31, 1988 - June 3, 1988, University of Colorado at Boulder, Colorado, Proceedings Volume (in print).

11. Nagabhushanam, J., Gaonkar, G.H., and Reddy, T.S.R., "Automatic Generation of Equations for Rotor-Body Systems with Dynamic Inflow for a Priori Ordering Schemes," Seventh European Rotorcraft and Powered Lift Aircraft forum, Garmisch-Partenkirchen, Federal Republic of Germany, Sept. 8-11, 1981, paper no. 37.

12. Crespo daSilva, M.R.M., and Hodges, D.H., "The Role of Computerized Symbolic Manipulation in Rotorcraft Dynamic Analysis", Computers and Mathematics with Applications, Vol. 12A, no. 1, 1986, pp. 161-172.

13. Reddy, T.S.R., and Warmbrodt, William, "Forward Flight Aeroelastic Stability from Symbolically Generated Equations", Journal of the American Helicopter Society, July 1986, pp. 35-44.

14. Xin, Zhao, and Curtiss, H.C., "A Linearized Model of Helicopter Dynamics including Correlation with Flight Test," Proceedings of the 2nd International Conference on Rotorcraft Basic Research, University of Maryland, February 16-18, 1988, pp. 2HAQ•1 - Zhao•14.

15. Done, G.T.S., Juggins, P.T.W., and Patel, M.H., "Further Experience with a New Approach to Helicopter Aeroelasticity, "Thirteenth European Rotorcraft Forum, Arles, France, Sept. 8-11, 1987, Paper No. 6•11.

16. Davenport, J.H., Siret, Y. and Tournier, E., Computer Algebra, Academic Press, New York, 1988.

17. Nagabhushanam, J., Gaonkar, G.H., Srinivasan, P., and Reddy, T.S.R., Users Manual for Automatic Generation of Equations of Motion and Damping Levels for Some Problems of Rotorcraft Flight Dynamics, R.&D. Report, HAL-IISc Helicopter Training Program, Indian Institute of Science, Bangalore, October 1984.

18. Reddy, T.S.R., "Symbolic Generation of Elastic Rotor Blade Equations Using a FORTRAN Processor and Numerical Study of Dynamic Inflow Effects on the Stability of Helicopter Rotors", NASA TM-86750, 1985.

19. Gaonkar, G. H., "Gust Response of Rotor and Propeller Systems," Journal of Aircraft, Vol. 18, No. 5, May 1981, pp. 389-396.

20. Lin, Y. K. and Prussing, J. E., "Concepts of Stochastic Stability in Rotor Dynamics," Journal of the American Helicopter Society, Vol. 27, No. 2, April 1982, pp. 73-74.

21. Prussing, J. E., Lin, Y. K. and Shiau, T-N., "Rotor Blade Flap-Lag Stability and Response in Forward Flight in Turbulend Flow," Journal of the American Helicopter Society, Vol. 29, No. 4, October 1984, pp. 81-87.

22. Peters, D. A., "Flap-Lag Stability of Helicopter Rotor Blades in Forward Flight," Journal of the American Helicopter Society, Vol. 20, No. 4, October 1975, pp. 2-13.

23. Prussing, J. E and Lin, Y. K., "Rotro Blade Flap-Lag Stability in Turbulent Flows," Journal American Helicopter Society, Vol. 27, No. 2, April 1982, pp. 51-57.

24. Prussing, J. E. and Lin, Y. K., "A Closed-Form Analysis of Rotor Blade Flap-Lag Stability In Hover and Low-Speed Forward Flight in Turbulent Flow," Journal of the American Helicopter Society, Vol. 28, No. 3, July 1983, pp. 42-46.

25. Lin, Y. K., "Structural Stability in Turbulent Flow," Recent Trends in Aeroelasticity, Structures and Structural Dynamics, Edited by P. Hajela, University Presses of Florida, Gainesville, 1987, pp. 259-268.

26. Lin, Y. K., Fujimori, Y and Ariaratnam, S. T., "Rotro Blade Stability in Turbulent Flows - Part I," AIAA Journal, Vol. 17, No. 6, June 1979, pp. 545-552.

27. Prussing, J. E., "Stabilization of an Unstable Linear System by Parametric White Noise," Journal of Applied Mechanics, Vol. 48, No. 1, March 1981, pp. 198-199.

28. Peters, D. A.," An Approximate Closed-Form Solution for Lead-Lad Damping of Rotor Blades in Hover," NASA TM X-62, 425, April 1975.

29. Gaonkar, G. H., "A Perspective on Modeling Rotorcraft in Turbulence," Journal of Probabilistic Engineering Mechanics, Vo. 3, No. 1, 1988, pp. 36-42.

30. Anderson, M. B., and Fordham, E. J., "An Analysis of Results from an Atmospheric Experiment to Examine the Structure of the Turbulend Wind as Seen by a Totating Observer," Cavendish Laboratory Report, Department of Physics University of Cambridge, U. K., 1982.

31. Dragt, J. B., "The Spectra of Wind Speed Fluctuations Met by Rotating Blade, and Resulting Load Fluctuations," European Wind Energy Conference 1984, Edited by Palz, W., Published by H. N. Stepens and Associates, pp. 453-458.

32. Holley, W. E., Thresher, R. W., and Lin, S. R. "Atmospheric Turbulence Inputs For Horizontal Axis Wind Turbines," European Wind Energy Conference 1984, Edited by Palz, W., Published by H. N. Stepens and Associates, pp. 453-458.

33. Talbot, P. D., Tinling, B. E., Decker, W. A. and Chen, R. T. N., A Mathematical Model of a Single Main Rotor Helicopter for Piloted Simulations, NASA TM-84281, September 1982, p. 7.

34. Elliot, A. S., and Chopra Inderjit, "Hingeless Rotor Response to Random Gusts in Forward Flight," AIAA Dynamics Specialists Conference, Monterey, California, 1987.

35. Nagabhushanam, J., Gaonkar, G. H. and McNulty, M. J., "An Experimental and Analytical Investigation of Stall Effects on Flap-Lag Stability in Forward Flight," Thirteenth European Rotorcraft Forum, Arles, France, September 8-11, 1987, Paper No. 6-2.

36. Bousman, W.G., and Ormiston, R.A., "A Study of Stall Induced Flap-Lag Instability of Hingeless Rotors," 19th Annual National Forum of the American Helicopter Society, Washington, D.C., May 1973, Preprint No. 730.

37. Peters, D.A., and Chouchane, M., "Effect of Dynamic Stall on Helicopter Trim and Flap-Lag Response, "Journal of Fluids and Structures, Vol. 1, 1987, pp. 299-318.